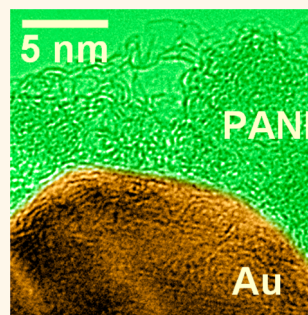


# Metallic Muscles at Work: High Rate Actuation in Nanoporous Gold/Polyaniline Composites

Eric Detsi, Patrick Onck, and Jeff Th. M. De Hosson\*

Department of Applied Physics, Zernike Institute for Advanced Materials, University of Groningen, Nijenborgh 4, 9747 AG Groningen, The Netherlands

**ABSTRACT** Metallic muscles made of nanoporous metals suffer from serious drawbacks caused by the usage of an aqueous electrolyte for actuation. An aqueous electrolyte prohibits metallic muscles from operating in dry environments and hampers a high actuation rate due to the low ionic conductivity of electrolytes. In addition, redox reactions involved in electrochemical actuation severely coarsen the ligaments of nanoporous metals, leading to a substantial loss in performance of the actuator. Here we present an electrolyte-free approach to put metallic muscles to work *via* a metal/polymer interface. A nanocoating of polyaniline doped with sulfuric acid was grown onto the ligaments of nanoporous gold. Dopant sulfate anions coadsorbed into the polymer coating matrix were exploited to tune the nanoporous metal surface stress and subsequently generate macroscopic dimensional changes in the metal. Strain rates achieved in the single-component nanoporous metal/polymer composite actuator are 3 orders of magnitude higher than that of the standard three-component nanoporous metal/electrolyte hybrid actuator.



**KEYWORDS:** nanoporous gold · polyaniline · electrolyte-free actuation

Metallic muscles<sup>1,2</sup> made of nanoporous metals with high surface area-to-volume ratios offer a unique combination of relatively large strain amplitudes, low operating voltages, high stiffness, and strength.<sup>3</sup> The challenge to their further development in viable applications can be considered three-fold but principally concerns the aqueous electrolyte that is needed to inject electronic charge in the space-charge region at the nanoporous metal/electrolyte interface.<sup>1</sup> Clearly, an aqueous electrolyte limits the usage of metallic muscles to wet environments, whereas most of the practical applications require artificial muscles that can operate in dry environments. A second, major concern is that the aqueous electrolyte limits the actuation rate because of its relatively low ionic conductivity.<sup>1</sup> Simply replacing the aqueous electrolyte by a solid one is an obvious solution, but the actuation rate of all-solid-state electrochemical actuators is more severely hampered by the low room-temperature ionic conductivity of solid-state electrolytes.<sup>1</sup> Completing the trio of challenges is the fact that the ligaments in nanoporous metals suffer from severe coarsening (undesired growth) during electrochemical processes,<sup>4</sup> including actuation *via* redox

reactions. Coarsening causes metallic muscles to lose performance after many cycles because the charge-induced strain is ligament-size-dependent, as shown in Supporting Information Figure S1. In addition to these technical boundaries, it is emphasized that metallic muscles operating as electrochemical actuators require a three-component configuration to function—explicitly, these are a working electrode, an electrolyte, and a counter electrode. In such a configuration, the working and counter electrodes, which may separately actuate as demonstrated by Kramer *et al.*,<sup>5</sup> are placed at a relatively large distance from each other.<sup>5,6</sup> This fixed distance represents a limitation for the integration of metallic muscles into miniaturized devices.<sup>7</sup> In view of these various restrictions caused by the electrolyte, an electrolyte-free approach is desirable in metallic muscles. In fact, the following features are a prerequisite for a breakthrough in the field of artificial muscles: (i) no usage of aqueous or solid electrolyte, (ii) a fast actuation rate, and (iii) a single actuating component as in piezoelectric materials. Regarding point (i), Biener *et al.*<sup>8</sup> and Detsi *et al.*<sup>9</sup> have recently reported on electrolyte-free actuation in nanoporous gold, based, respectively, on the chemical

\* Address correspondence to j.t.m.de.hosson@rug.nl.

Received for review February 17, 2013 and accepted April 12, 2013.

Published online April 12, 2013  
10.1021/nn400803x

© 2013 American Chemical Society

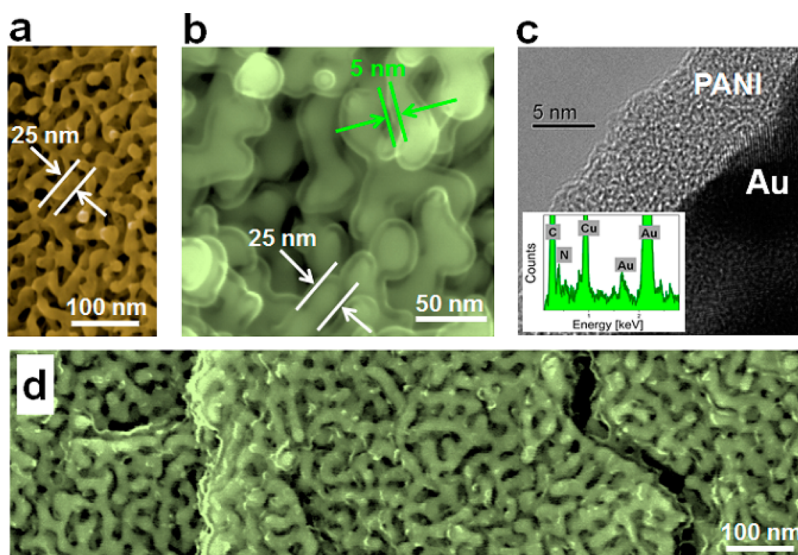


**Figure 1.** Microstructural characterization of NPG/PANI. (a) Scanning electron micrograph showing the bicontinuous morphology of NPG. (b,c) Scanning and transmission electron micrographs showing a  $\sim 5$  nm thick PANI skin covering the ligaments of NPG. The inset of c displays the EDX spectrum of PANI. C and N come from aniline ( $C_6H_7N$ ); Cu and Au come, respectively, from the Cu grid used as sample holder and the NPG. (d) Fracture cross section of NPG/PANI. It can be seen that the polymer envelope covering the ligaments is present in the bulk of the composite material.

adsorption and the physical adsorption of gas molecules at the nanoporous metal/gas interface. However, the response rate of nanoporous gold/gas composite actuators is low. Here we present a novel approach to generate work from metallic muscles that navigates all three of the above-mentioned hurdles. When metallic muscles are put to work *via* an aqueous electrolyte, an electrical voltage is used to modulate their surface stress by tuning the interfacial electronic charge density in a space-charge region at the nanoporous metal/electrolyte interface.<sup>2,3,5,6,10</sup> Rather than a nanoporous metal/electrolyte composite material, here we generate work from a metal by exploiting a bulk hybrid material consisting of nanoporous metal and polymer coating grown onto the ligaments of the nanoporous metal. In this article, we used nanoporous gold (NPG) as the metallic muscle and polyaniline (PANI) as the polymer envelope (skin) to show the proof of principle.

## RESULTS AND DISCUSSION

### Synthesis and Microstructural Characterization of NPG/PANI.

NPG was synthesized by the standard dealloying method (see Supporting Information).<sup>6,11</sup> The typical bicontinuous morphology of the synthesized NPG is shown on the scanning electron micrograph of Figure 1a. The corresponding interface surface area per unit mass computed from the analytical expression for the specific surface area of nanoporous materials<sup>11–14</sup> was found to be  $\sim 7.7$  m<sup>2</sup> g<sup>-1</sup>. The internal surface area of the three-dimensional bicontinuous network of the synthesized NPG was uniformly coated by an electropolymerization procedure, and a continuous doped polymer envelope covers the ligaments.<sup>15,16</sup>

The potentiodynamic procedure (*i.e.*, monomer deposition with a variable voltage *via* cyclic voltammetry) was used,<sup>17</sup> and the polymerization of aniline was carried out from an aqueous solution containing 50 mM of aniline monomer and 0.5 M of H<sub>2</sub>SO<sub>4</sub> used as solvent and dopant molecules.<sup>15</sup> Details on electropolymerization are added in the Methods. The scanning and transmission electron micrographs of Figure 1b,c, respectively, display a uniform PANI skin with an average thickness of  $\sim 5$  nm grown onto the ligaments of NPG. The presence of carbon and nitrogen as constituents of the organic coating monomer C<sub>6</sub>H<sub>7</sub>N (aniline) was confirmed from energy-dispersive X-ray spectroscopy (EDS) performed during characterization of the PANI film by transmission electron microscopy (TEM). The typical EDS spectrum of this PANI envelope is displayed in the inset of Figure 1c. In this energy spectrum, the Cu and Au peaks are, respectively, attributed to the Cu grid used as the sample holder and to the NPG. The scanning electron micrograph of Figure 1d represents a fracture cross section of the NPG/PANI hybrid material. It can be seen that the nanocoating of polymer covering the ligaments of NPG is present in the bulk of the material.

### Nature of Electronic Charge Transport in the Polymer Skin.

The knowledge of the nature of electronic charge transport in the PANI film is necessary for a better insight into the actuation mechanism in the NPG/PANI hybrid material. A schematic illustration of this NPG/PANI bulk heterojunction actuator is shown in Figure 2a–d, and additional technical details are found in Supporting Information. The actuator is connected to the voltage supplier in one of the following two configurations: NPG/PANI/Au with NPG as anode and

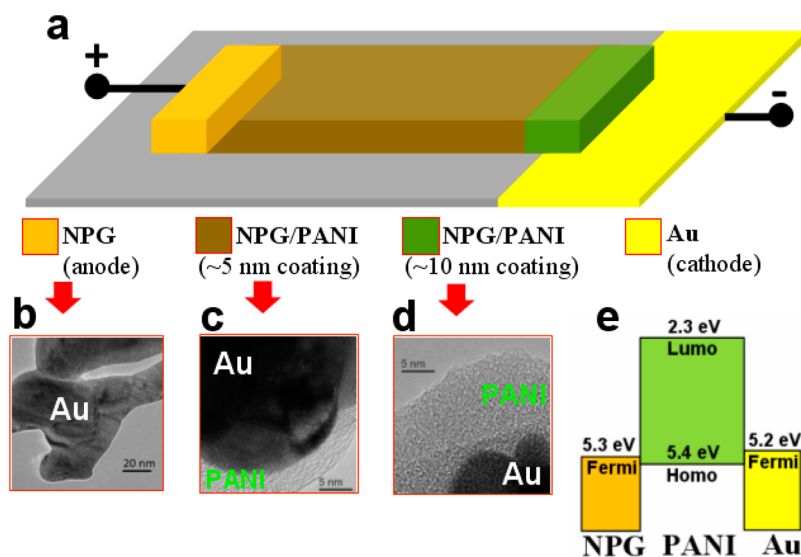


**Figure 2.** NPG/PANI bulk junction actuator. (a,c) Main part of the actuator consists of NPG whose ligaments are coated with a  $\sim 5$  nm layer of PANI. (b) One edge connected to the positive terminal of the voltage supplier consists of NPG; (d) other edge connected to the negative terminal consists of NPG having its ligaments covered with  $\sim 10$  nm thick layer of PANI. (e) Energy-level diagram of the system NPG/PANI/Au system in the absence of an applied potential.

solid Au as cathode (see Figure 2a), or Au/PANI/NPG with solid Au as anode and NPG as cathode. Both configurations can be used because the two contact electrodes (NPG and solid Au) are made of the same material. It is emphasized with respect to Figure 2a that the NPG/PANI junction is a 3D bulk contact, whereas the PANI/Au junction is a 2D contact. Although the effective contact areas between these two junctions are different (NPG/PANI area  $\gg$  PANI/Au area), the electrical conductivity between the two gold electrodes (*i.e.*, NPG and Au from Figure 2a) was found to be very good. This is justified by the fact that PANI is a heavily doped semiconductor, with a very good electrical conductivity.

Since the work functions of NPG and solid Au are comparable with the highest occupied molecular orbital (HOMO) of PANI on the one hand,<sup>18</sup> and since PANI is a p-type semiconductor on the other hand,<sup>19</sup> electronic charge transport in the NPG/PANI hybrid actuator is only controlled by hole conduction rather than by both electron and hole transports. Such a single carrier system is commonly referred to as a “hole-only” device because the high offset between the Fermi level of the metal and the lowest unoccupied molecular orbital (LUMO) of PANI restricts electron injection from the metal into the LUMO of the polymer at low voltages.<sup>20</sup> The energy-level diagram of the NPG/PANI/Au system in the absence of an applied potential is shown in Figure 2e; it is seen that holes can readily be injected from the anode into the HOMO of PANI.

An external electric potential was used to inject holes from the metal anode (either NPG or solid Au) into the HOMO of the PANI envelope.<sup>21</sup> A particularity of the NPG/PANI/Au or Au/PANI/NPG configuration is that electronic charges injected from the anode must

flow through the PANI film before reaching the cathode. The typical current density–voltage ( $J$ – $V$ ) characteristic of the Au/PANI/NPG system (hole injection from Au) is shown on the semi-logarithmic plot of Figure 3a for three successive forward–backward voltage sweeps (from 0 to 2 V and back to 0 V). The inset of Figure 3a displays the corresponding forward  $J$ – $V$  curve on a double logarithmic graph. Similarly, the  $J$ – $V$  curve of the NPG/PANI/Au system (hole injection from NPG) is shown on the semi-logarithmic plot of Figure 3b for three successive forward–backward voltage sweeps in the same potential range between 0 and 2 V. The inset of Figure 3b displays the corresponding forward  $J$ – $V$  curve on a double logarithmic plot. The hysteresis<sup>22</sup> in the  $J$ – $V$  curves is more pronounced when holes are injected from solid Au (Figure 3a) than from NPG (Figure 3b); this can be caused by the above-mentioned difference in contact area for hole injection, which is larger for the NPG/PANI interface than the Au/PANI interface. Irrespective of this difference, it can be concluded from the slope values of 1 obtained on the double logarithmic graphs for both NPG/PANI/Au and Au/PANI/NPG configurations (see insets of Figure 3a,b) that, at low potentials, electronic charge transport through the polymer skin follows an Ohmic behavior at ambient temperatures.<sup>23,24</sup> A similar Ohmic behavior is commonly reported when the two contact electrodes are made of solid Au in the following configuration:<sup>18</sup> Au/PANI/Au. It is emphasized that the Ohmic nature of the current in the NPG/PANI hybrid actuator means that electronic charges do not accumulate at the metal/polymer interface during potential sweeps, as it is the case at a metal/electrolyte interface, where the (pseudo)capacitive double layer formed at this

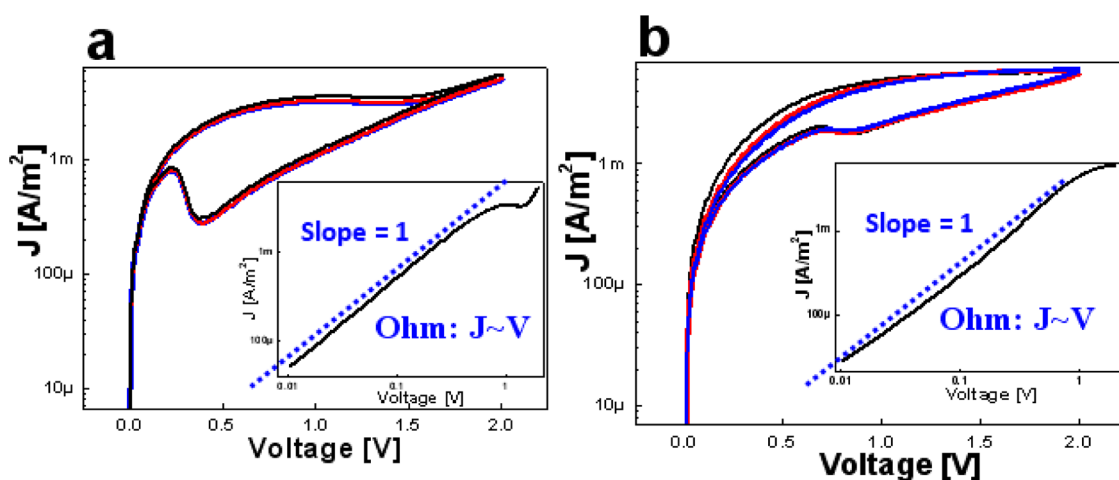


**Figure 3.** Nature of electronic charge transport in the PANI skin. Semi- and double (insets) logarithmic plots of the  $J$ – $V$  curves for three successive forward–backward voltage cycles. It can be seen from the slope values of 1 that hole transport in the PANI coating follows an Ohmic behavior in the potential range between 0 and 2 V. (a) Hole injection from Au for the Au/PANI/NPG configuration. (b) Hole injection from NPG for the NPG/PANI/Au configuration.

metal/electrolyte interface is exploited for actuation.<sup>2</sup> Therefore, the approach presented in this article for the modulation of the electronic charge density at the NPG/PANI interface is different from the building up of space-charge encountered in nanoporous metal/electrolyte hybrid systems.

#### Electrolyte-Free Actuation in the NPG/PANI Hybrid Material.

Reversible dimensional changes were recorded in the NPG/PANI bulk heterojunction material during successive forward–reverse voltage cycles between 0 and 2 V and at various sweep rates ranging from 1 to 2000 mV/s. A confocal displacement sensor (IFS2401-0.4 Micro-Epsilon) was used for this purpose.<sup>6</sup> Figure 4 displays typical dimensional changes as a function of the time recorded during 50 successive forward–backward potential sweeps at the sweep rate of 10 mV/s for the Au/PANI/NPG configuration. The NPG/PANI hybrid material expands during the forward sweep and contracts during the reverse process. The sign of the displacement is reversed when the actuator is connected in the NPG/PANI/Au configuration (*i.e.*, contraction during forward sweep and expansion during backward sweep). Fifty well-reproducible expansion–contraction cycles are recorded in response to 50 forward–reverse voltage cycles. The strain amplitude at the sweep rate of 10 mV/s is on the order of  $\sim 0.15\%$ , and this is comparable to the one reported at lower sweep rates (between 0.2 and 1 mV/s) in nanoporous metal/electrolyte composites.<sup>2,10</sup> Note that in Figure 4, the drifting of the background comes from the fact that strain measurements were performed in a noncontact mode; that is, the moving NPG/PANI sample is free-standing. Consequently, the slightly curved NPG/PANI strip (the curvature in the strip comes from the volume contraction in NPG during dealloying<sup>6</sup>) is not perfectly flat on the support. As a result, in addition to the reversible charge-induced dimensional changes in the NPG/PANI composite, the

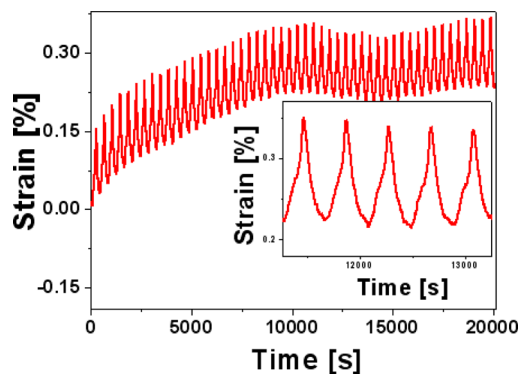


**Figure 4.** Electrolyte-free actuation in NPG/PANI. Fifty well-reproducible expansion–contraction cycles recorded in response to 50 successive forward–reverse  $J$ – $V$  cycles in the Au/PANI/NPG configuration. The NPG/PANI hybrid material expands during the forward sweep and contracts during the reverse process.

bent strip also “vibrates” a bit during many successive actuation cycles.

It is emphasized that low sweep rates are required during actuation in nanoporous metals *via* an electrolyte; in fact, dimensional changes in nanoporous metal/electrolyte composite actuators vanish at sweep rates beyond a few tens of mV/s. That behavior has two origins: (i) the low room-temperature ionic conductivity of electrolytes<sup>1,10,25</sup> does not favor a rapid transport of ions to the nanoporous metal/electrolyte interface; (ii) the equilibration of redox reactions involved in charge transferred at the nanoporous metal/electrolyte interface is not satisfied during fast sweep rates as highlighted in ref 10.

The impact of the voltage sweep rate on the performance of metallic muscles is clearly illustrated in the work of Viswanath *et al.*,<sup>10</sup> who reported on a decrease of the strain amplitude in the nanoporous metal/electrolyte composite actuator from  $\sim 0.14$  to 0.05%

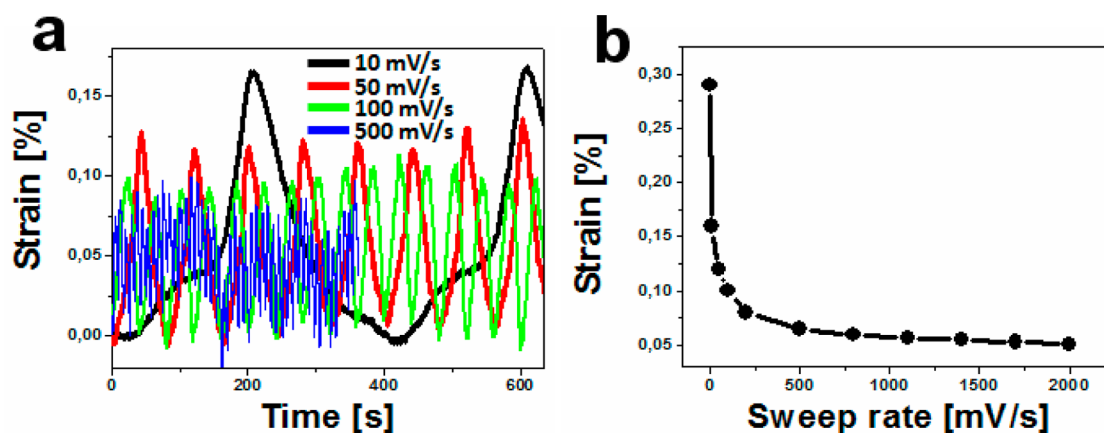
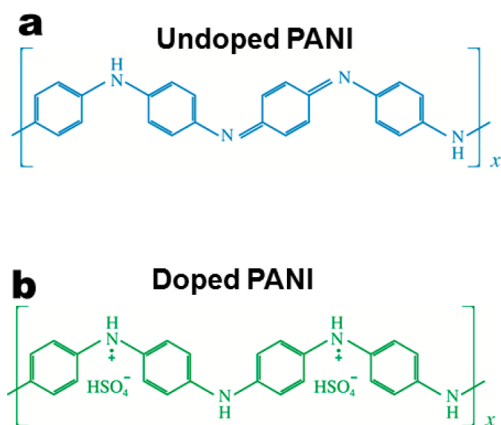


Figure 5. Fast actuation responses. Reversible dimensional changes are recorded at various sweep rates far beyond 1 mV/s (a) as a function of the time and (b) as a function of the sweep rate.

when the sweep rate is increased from 30  $\mu\text{V/s}$  to 1 mV/s. That strain amplitude of  $\sim 0.05\%$  is achieved in 1400 s with the electrolyte,<sup>10</sup> which corresponds to a strain rate of  $3.6 \times 10^{-7}$  per second. For the sake of comparison, a mammalian skeletal muscle has a strain rate of  $\sim 10^{-1}$  per second<sup>1</sup> and is able to achieve the 0.05% strain amplitude in 5 ms; most artificial muscles have their strain rate ranging between  $\sim 10^{-3}$  and  $10^{-1}$  per second.<sup>26</sup> In contrast to metallic muscles operating in electrolytes where dimensional changes are not present at sweep rates beyond a few tens of mV/s, reversible dimensional changes were still observed in our NPG/PANI electrolyte-free actuator at sweep rates far beyond 1 mV/s, as illustrated in Figure 5a,b, where the strain amplitudes are plotted as a function of the time and sweep rate, respectively. By setting the sweep rate at 2000 mV/s, the aforementioned strain of  $\sim 0.05\%$  was achieved in our electrolyte-free actuator in 1 s, rather than 1400 s as with the electrolyte.<sup>10</sup> This corresponds to a strain rate of  $5 \times 10^{-4}$  per second, which is thus about 1400 times higher than that achieved in metallic muscles *via* an electrolyte. These results demonstrate that, by virtue of the novel electrolyte-free actuation approach, metallic muscles can operate in dry environments at high strain rates, much higher than those of common electrochemical artificial muscles.

**Origin of Dimensional Changes in the NPG/PANI Hybrid Material.** Referring to the nanoporous metal/electrolyte hybrid actuator, it is well-established that dimensional changes in this system are caused by changes in the nanoporous metal surface stress when electronic charges are injected at the nanoporous metal/electrolyte interface during ion electro-adsorption,<sup>2,3,5,6,10</sup> in order to preserve the mechanical equilibrium,<sup>27</sup> these changes in the nanoporous metal surface stress are compensated by opposite changes in the stress state in the bulk of the ligaments, resulting in overall macroscopic dimensional changes in the nanoporous metal.<sup>2,3,5,6,10,27</sup> For our NPG/PANI hybrid material, the

situation is different because no electrolyte is used during actuation. In the absence of an electrolyte, changes in the NPG surface stress as a result of electronic charge accumulation in the space-charge region at the NPG interface are still possible, provided that an opposite space-charge builds up in the polymer coating during the voltage sweeps. However, as we have seen in a previous section, hole transport in the PANI coating is governed by an Ohmic current (slope value of 1 in the double logarithmic plot), rather than a space-charge-limited current (slope value of 2 in the double logarithmic plot).<sup>28</sup> This rejects the possibility of having changes in the surface stress of NPG as result of the building up of a space-charge in the polymer coating. Another possible origin of the measured dimensional changes in the NPG/PANI hybrid material points toward actuation in PANI. First, PANI can undergo reversible dimensional changes during electrochemical oxidation/reduction.<sup>29</sup> However, this option is not applicable to our electrolyte-free actuator because the electrochemical oxidation/reduction of PANI requires an electrolyte. Second, charge carriers in conducting polymers including PANI are susceptible to inducing conformational changes in the polymer chains.<sup>30–33</sup> This later deformation mode does not necessarily require the oxidation or reduction of the polymer.<sup>30</sup> Conformational changes in PANI chains can therefore be responsible for the dimensional changes in our NPG/PANI composite material, provided that stresses developed in the polymer chains during these conformational changes are fully transferred to the metal. This is less likely the case because the mechanical adhesion at metal/polymer interfaces is commonly weak.<sup>34</sup> In addition, the relatively small PANI content in the NPG/PANI composite material ( $\sim \text{Au}_{95}(\text{PANI})_5$  wt %) and the relatively small Young's modulus of PANI ( $\sim 2$  GPa),<sup>35</sup> compared to that of the metallic ligaments ( $\sim 79$  GPa), lead to a reasonable conclusion that the measured strains in our composite material do not come from actuation in the thin polyaniline coating.



**Figure 6.** Charges present in doped PANI chains. (a) Undoped PANI, blue insulating emeraldine base. (b) Doped PANI, green conducting emeraldine salt. Free radicals, positive charges (polymeric cations), and sulfate counterions are present in doped PANI chains. These sulfate counterions are responsible for actuation.

We propose the following picture for the origin of the dimensional changes recorded in our NPG/PANI hybrid material. As schematized in Figure 6a, the nonconducting form of PANI (blue emeraldine base) consists of electrically neutral molecular chains.<sup>36</sup> PANI is made conducting (green emeraldine salt) by protonic acid doping or oxidative doping. The removal of electrons from the  $\pi$ -conjugated backbone of PANI during oxidative doping gives rise to free radicals and positive charges (polymeric cations) as schematized in Figure 6b. In the case of sulfuric acid doping,<sup>36</sup> the charge neutrality in the doped PANI is maintained by negative sulfate counterions coadsorbed into the polymer matrix during the doping process.<sup>30,37</sup> Both polymer cations and sulfate counterions along a doped PANI chain are held together by electrostatic interactions.<sup>38</sup> When a suitable electrical potential is applied on the NPG/PANI hybrid actuator, the positive charges on the  $\pi$ -conjugated backbone of PANI become involved in electrical conduction, whereas the negative sulfate counterions remain localized along the chains. During potential sweeps, sulfate counterions dispersed into the thin PANI matrix electrostatically interact with the NPG electrode.<sup>30</sup> PANI molecular chains eventually undergo conformational changes in order to bring (or take away) sulfate anions in the proximity of the positive (or negative) NPG electrode; sulfate anions present in the first monolayer of PANI are eventually electro-adsorbed onto the gold electrode as reported by Lee *et al.*<sup>30</sup> Note that the key point in this process is the electrical potential-induced interactions between the gold substrate and sulfate ions from the PANI coating.<sup>30</sup> Obviously, these interactions between sulfate counterions and the metal electrode also give rise to charge-induced relaxation (or contraction) of the metal surface.<sup>39</sup> As a consequence of the high surface area-to-volume ratio of the

NPG substrate, onto which PANI is grown, the charge-induced relaxation (or contraction) of the NPG interface results in macroscopic dimensional changes in this NPG.<sup>6,27</sup> The total amount of negative charges in the polymer matrix, arising from coadsorbed sulfate counterions, was estimated in the case of a 5 nm thick PANI coating and was found to be  $\sim 3.2$  C per  $\text{m}^2$  coating, assuming that each repeating unit of PANI contributes with two sulfate anions, as illustrated in Figure 6b. This amount of charge is comparable to the quantity of electronic charge involved in dimensional changes in nanoporous metal/electrolyte hybrid actuators.<sup>10</sup> This supports our argument on the origin of the measured dimensional changes, which we have attributed to the relaxation (contraction) of the high surface area-to-volume ratio NPG substrate when coadsorbed dopant counterions present in the PANI coating matrix interact with this NPG substrate upon application of an external potential.

Although the dimensional changes in the NPG/PANI hybrid actuator do not come from actuation in PANI, it is believed that conformational changes in the polymer chains play an important role during actuation: (i) conformational changes (*i.e.*, changes in the molecular shapes of PANI chains) take place, in order bring sulfate anions in the proximity of the metal electrode.<sup>30</sup> This process can be compared with the diffusion ions toward a metal/electrolyte interface in the case of actuation in a nanoporous metal/aqueous electrolyte system. (ii) The high rate of which conducting polymers undergo conformational changes as highlighted by Yip and co-workers<sup>32</sup> might justify the high actuation rate recorded on our NPG/PANI composite: rapid shape changes in polymer chains favor a fast exposure (removal) of sulfate anions to the NPG electrode. In contrast, when ions are transported through an electrolyte, a high actuation rate is hampered because of the low ionic conductivity of electrolytes.<sup>1,25</sup> Note that the response rate of the NPG/PANI actuator is still lower than that of piezoceramics or some polymer actuators.<sup>26</sup> It is believed that this response rate can be optimized by tailoring the concentration of the dopant counterions in the polymer: the more charges (counterions) present in the polymer matrix, the higher the charge-induced strain and the corresponding strain rate. The combination of NPG with other conducting polymers, such as polypyrrole (PPy),<sup>16</sup> may also be envisaged in order to further investigate the response rate.

**Work Density.** The work density  $W = 1/2Y\epsilon^2$  of the NPG/PANI actuator ( $\sim 113$  kJ/m<sup>3</sup>; see Supporting Information) is comparable to the  $\sim 130$  kJ/m<sup>3</sup> achieved in piezoceramics<sup>3</sup> and 90 kJ/m<sup>3</sup> reported for the nanoporous metal/electrolyte actuator in ref 2. However, it is noteworthy to specify that this work density is still at least 1 order of magnitude lower than the highest work densities reported so far in nanoporous metal actuators.<sup>3,6</sup> In the above expression,  $W$ ,  $Y$ ,

and  $\varepsilon$  represent the volume work density, effective Young's modulus, and maximum strain amplitude, respectively.<sup>6,40</sup> Nonetheless, although the work density is the standard measure for the mechanical performance of artificial muscles, it is pointed out that a high value of  $W$  does not necessarily mean that the corresponding actuation material is suitable for every application. In fact, each actuation material satisfies only specific applications depending on how  $Y$  and  $\varepsilon$  are combined: materials such as electroactive polymers can produce large actuation strokes ( $\varepsilon \sim 4.5\%$ ), but they are weak ( $Y \sim 1.1$  GPa);<sup>3</sup> others like piezoceramics are strong ( $Y \sim 64$  GPa), but their strain amplitudes are restricted to  $\sim 0.2\%$ .<sup>3</sup> Metallic muscles are unique for a number of reasons, but none more so than in the sense that they can achieve a wide range of strengths as depicted by the effective Young's modulus of NPG, which is tunable from  $\sim 5$  to  $\sim 45$  GPa through manipulation of the ligaments' size.<sup>41</sup> Additionally, they can also be designed to achieve a wide window of strain amplitudes ranging from the standard value of  $\sim 0.1\%$  up to large strains of  $\sim 1.3\%$  in binary nanoporous alloys<sup>3</sup> and  $\sim 6\%$  in nanoporous metals with a dual microscopic length scale structure.<sup>6</sup> Furthermore, they operate at low voltages compared to common artificial muscles. Despite these unique features, the emergence of nanoporous metal actuators in practicable applications is still delayed, a decade after their discovery.<sup>2</sup> The reasons for this are the drawbacks

discussed in this article. Exploiting a polymer skin augmentation of the muscle for actuation, as we have demonstrated, is expected to stimulate the development of metallic muscles into a new class of actuation materials that operate at low voltages and combine large strain amplitudes with high stiffness and strength.<sup>3</sup>

## CONCLUSIONS

In conclusion, we have demonstrated a new electrolyte-free approach to generate work from nanoporous metals by exploiting a nanoporous metal/polymer interface, rather than the common nanoporous metal/electrolyte interface. In this actuation concept, a doped polymer coating is grown onto the ligaments of the nanoporous metal and dopant counterions present in the polymer coating matrix are exploited to modulate the nanoporous metal surface stress, which results in dimensional changes in the nanoporous metal. In our actuation concept, the various drawbacks encountered with metallic muscles operating in aqueous electrolytes have been overcome. In particular, our electrolyte-free actuator consists of a single-component hybrid material, in contrast to the three-component configuration required in nanoporous metal/electrolyte composite actuators; the actuation rate of the nanoporous metal/polymer hybrid actuator is about 3 orders of magnitude higher than that of metallic muscles operating in aqueous electrolytes.

## METHODS

**Electropolymerization.** The deposition of a nanocoating of PANI onto the ligaments of NPG was achieved by electrochemical oxidative polymerization of aniline from an aqueous solution containing aniline monomers. The potentiodynamic procedure (monomers deposition with a variable voltage *via* cyclic voltammetry) was used. These cyclic voltammetry experiments were carried out using a potentiostat  $\mu$ Autolab III-FRA2, Eco Chemie,<sup>6</sup> and a three-electrode electrochemical cell containing 0.5 M of  $\text{H}_2\text{SO}_4$  and 50 mM of aniline monomers. The  $\sim 5$  nm PANI coating in Figures 1b and 2c was achieved after 15 successive cyclic voltammetry experiments in the potential range between  $-0.2$  and  $1.2$  V measured with respect to a Ag/AgCl reference electrode. Following this step, the sample was partially removed from the electrochemical cell, leaving only the edge in contact with the electrolyte for further electropolymerization. This allows the formation of a thicker PANI coating after 20 additional cycles ( $\sim 10$  nm; see Figure 2d). The thick PANI coating is required for the connection of the actuator with the voltage supplier. It is pointed out that the conducting form of PANI is a heavily doped semiconductor, with a very good electrical conductivity. This justifies why an electrical contact is easily made between the thick PANI coating and a solid gold electrode (*i.e.*, contact between the green and yellow edges in Figure 2a). Note that, during the entire electropolymerization process, the upper part of the NPG sample is not immersed in the electrolyte because a polymer-free NPG edge is required during actuation to inject a hole into the polymer (see Figure 2b).

**Conflict of Interest:** The authors declare no competing financial interest.

**Acknowledgment.** The authors are grateful to The Netherlands Organization for Scientific Research (NWO-the Hague, Mozaïek

2008 BOO Dossiernr: 017.005.026) and the Zernike Institute for Advanced Materials for their financial support.

**Supporting Information Available:** Preparation of the alloy precursor and dealloying; technical details about the NPG/PANI actuator; estimation of the work density; Figure S1 showing the size-dependent charge-induced strain in NPG/electrolyte composites. This material is available free of charge *via* the Internet at <http://pubs.acs.org>.

## REFERENCES AND NOTES

- Baughman, R. H. Muscles Made from Metal. *Science* **2003**, *300*, 268–269.
- Weissmüller, J.; Viswanath, R. N.; Kramer, D.; Zimmer, P.; Würschum, R.; Gleiter, H. Charge-Induced Reversible Strain in a Metal. *Science* **2003**, *300*, 312–315.
- Jin, H. J.; Wang, X.-L.; Parida, S.; Wang, K.; Seo, M.; Weissmüller, J. Nanoporous Au–Pt Alloys as Large Strain Electrochemical Actuators. *Nano Lett.* **2010**, *10*, 187–194.
- Zhang, J.; Liu, P.; Ma, H.; Ding, Y. Nanostructured Porous Gold for Methanol Electro-Oxidation. *J. Phys. Chem. C* **2007**, *111*, 10382–10388.
- Kramer, D.; Viswanath, R. N.; Weissmüller, J. Surface-Stress Induced Macroscopic Bending of Nanoporous Gold Cantilevers. *Nano Lett.* **2004**, *4*, 793–796.
- Detsi, E.; Punzhin, S.; Rao, J.; Onck, P. R.; De Hosson, J. T. M. Enhanced Strain in Functional Nanoporous Au with a Dual Microscopic Length Scale Structure. *ACS Nano* **2012**, *6*, 3734–3744.
- Conway, N. J.; Traina, Z. J.; Kim, S. G. A Strain Amplifying Piezoelectric MEMS Actuator. *J. Micromech. Microeng.* **2007**, *17*, 781.
- Biener, J.; Wittstock, A.; Zepeda-Ruiz, L. A.; Biener, M. M.; Zielasek, V.; Kramer, D.; Viswanath, R. N.; Weissmüller, J.

- Bäumer, M.; Hamza, A. V. Surface-Chemistry-Driven Actuation in Nanoporous Gold. *Nat. Mater.* **2009**, *8*, 47–51.
9. Detsi, E.; Chen, Z. G.; Vellinga, W. P.; Onck, P. R.; De Hosson, J. T. M. Reversible Strain by Physisorption in Nanoporous Gold. *Appl. Phys. Lett.* **2011**, *99*, 083104.
10. Viswanath, R. N.; Kramer, D.; Weissmüller, J. Adsorbate Effects on the Surface Stress- Charge Response of Platinum Electrodes. *Electrochim. Acta* **2008**, *53*, 2757–2767.
11. Detsi, E.; De Jong, E.; Zinchenko, A.; Vuković, Z.; Vuković, I.; Punzhin, S.; Loos, K.; Ten Brinke, G.; De Raedt, H. A.; Onck, P. R.; *et al.* On the Specific Surface Area of Nanoporous Materials. *Acta Mater.* **2011**, *59*, 7488–7497.
12. Tan, Y. H.; Davis, J. A.; Fujikawa, K.; Ganesh, N. V.; Demchenko, A. V.; Stine, K. J. Surface Area and Pore Size Characteristics of Nanoporous Gold Subjected to Thermal, Mechanical, or Surface Modification Studied Using Gas Adsorption Isotherms, Cyclic Voltammetry, Thermogravimetric Analysis, and Scanning Electron Microscopy. *J. Mater. Chem.* **2012**, *22*, 6733–6745.
13. Detsi, E.; Vuković, Z.; Punzhin, S.; Bronsveld, P. M.; Onck, P. R.; De Hosson, J. T. M. Fine-Tuning the Feature Size of Nanoporous Silver. *CrystEngComm.* **2012**, *14*, 5402–5406.
14. Detsi, E.; Punzhin, S.; Onck, P. R.; De Hosson, J. T. M. Direct Synthesis of Metal Nanoparticles with Tunable Porosity. *J. Mater. Chem.* **2012**, *22*, 4588–7591.
15. Lang, X.; Zhang, L.; Fujita, T.; Ding, Y.; Chen, M. Three-Dimensional Bicontinuous Nanoporous Au/Polyaniline Hybrid Films for High-Performance Electrochemical Supercapacitors. *J. Power Sources* **2012**, *197*, 325–329.
16. Meng, F.; Ding, Y. Sub-Micrometer-Thick All-Solid-State Supercapacitors with High Power and Energy Densities. *Adv. Mater.* **2011**, *23*, 4098–4102.
17. Heinze, J.; Frontana-Urbe, B. A.; Ludwigs, S. Electrochemistry of Conducting Polymers—Persistent Models and New Concepts. *Chem. Rev.* **2010**, *110*, 4724.
18. Reis, F. T.; Santos, L. F.; Faria, R. M.; Mencaraglia, D. Temperature Dependent Impedance Spectroscopy on Polyaniline Based Devices. *IEEE Trans. Dielectr. Electr. Insul.* **2006**, *13*, 1074.
19. Bhadra, S.; Khastgir, D.; Singha, N. K.; Lee, J. H. Progress in Preparation, Processing and Applications of Polyaniline. *Prog. Polym. Sci.* **2009**, *34*, 783–810.
20. Parker, I. D. Carrier Tunneling and Device Characteristics in Polymer Light-Emitting Diodes. *J. Appl. Phys.* **1994**, *75*, 1656.
21. Shen, Y.; Hosseini, A. R.; Wong, M. H.; Malliaras, G. G. How To Make Ohmic Contacts to Organic Semiconductors. *ChemPhysChem* **2004**, *5*, 16–25.
22. Craciun, N. I.; Zhang, Y.; Palmaerts, A.; Nicolai, H. T.; Kuik, M.; Kist, R. J. P.; Wetzelaer, G. A. H.; Wildeman, J.; Vandenberg, J.; Lutsen, L.; *et al.* Hysteresis-Free Electron Currents in Poly(*p*-phenylene vinylene) Derivatives. *J. Appl. Phys.* **2010**, *107*, 124504.
23. Kronemeijer, A. J.; Huisman, E. H.; Katsouras, I.; van Hal, P. A.; Geuns, T. C. T.; Blom, P. W. M.; Van de Molen, S. J.; De Leeuw, D. M. Universal Scaling in Highly Doped Conducting Polymer Films. *Phys. Rev. Lett.* **2010**, *105*, 156604.
24. Blom, P. W. M.; Vissenberg, M. C. J. M. Charge Transport in Poly(*p*-phenylene vinylene) Light-Emitting Diodes. *Mater. Sci. Eng.* **2000**, *27*, 53–94.
25. Allebrod, F.; Mollerup, P. L.; Chatzichristodoulou, C.; Mogensen, M. B. Electrical Conductivity Measurements of Aqueous and Immobilized Potassium Hydroxide. *Int. J. Hydrogen Energy* **2012**, *37*, 16505–16514.
26. Madden, J. D.; Cush, R. A.; Kanigan, T. S.; Hunter, I. W. Fast Contracting Polypyrrole Actuators. *Synth. Met.* **2000**, *113*, 185–192.
27. Jin, H.-J.; Weissmüller, J. Bulk Nanoporous Metal for Actuation. *Adv. Eng. Mater.* **2010**, *12*, 714–723.
28. Blom, P. W. M.; De Jong, M. J. M.; Vleggaar, J. J. M. Electron and Hole Transport in Poly(*p*-phenylene vinylene) Devices. *Appl. Phys. Lett.* **1996**, *68*, 3308.
29. Yan, H.; Tomizawa, K.; Ohno, H.; Toshima, N. All-Solid Actuator Consisting of Polyaniline Film and Solid Polymer Electrolyte. *Macromol. Mater. Eng.* **2003**, *288*, 578–584.
30. Lee, Y. H.; Chang, C. Z.; Yau, S. L.; Fan, L. J.; Yang, Y. W.; Yang, L. Y. O.; Itaya, K. Conformation of Polyaniline Molecules Adsorbed on Au(111) Probed by *In Situ* STM and *Ex Situ* XPS and NEXAFS. *J. Am. Chem. Soc.* **2009**, *131*, 6468–6474.
31. Botelho, A. L.; Lin, X. Soliton and Polaron Induced 3D Conformational Changes in Conjugated Polymers. *Am. Phys. Soc. Meeting* **2009**, *54*, (<http://meetings.aps.org/link/BAPS.2009.MAR.H20.2>).
32. Lin, X.; Li, J.; Yip, S. Controlling Bending and Twisting of Conjugated Polymers *via* Solitons. *Phys. Rev. Lett.* **2005**, *95*, 198303.
33. Lin, X.; Li, J.; Smela, E.; Yip, S. Polaron-Induced Conformation Change in Single Polypyrrole Chain: An Intrinsic Actuation Mechanism. *Int. J. Quantum Chem.* **2005**, *102*, 980–985.
34. Vellinga, W.-P.; Detsi, E.; Hosson, J. D. 3D-Effects on Delamination Along Polymer-Metal Interfaces. *Mater. Res. Soc. Symp. Proc.* **2008**, *1116*, 37–42.
35. Meixiang, W.; Lijuan, L.; Jun, W. Electrical and Mechanical Properties of Polyaniline Films—Effect of Neutral Salts Added. *Chin. J. Polym. Sci.* **1998**, *16*, 1–8.
36. Krinichnyi, V. I.; Roth, H.-K.; Hinrichsen, G.; Lux, F.; Lüders, K. EPR and Charge Transfer in H<sub>2</sub>SO<sub>4</sub>-Doped Polyaniline. *Phys. Rev. B* **2002**, *65*, 155205.
37. Nahar, M. S.; Zhang, J. Charge Transfer in Anion Doped Polyaniline. *International Conference on Signal, Image Processing and Applications, IPCSIT*; IACSIT Press: Singapore, 2011; p 21.
38. Choi, M.-R.; Woo, S. H.; Han, T. H.; Lim, K. G.; Min, S. Y.; Yun, W. M.; Kwon, O. K.; Park, C. E.; Kim, K. D.; Shin, H. K.; *et al.* Polyaniline-Based Conducting Polymer Compositions with a High Work Function for Hole-Injection Layers in Organic Light-Emitting Diodes: Formation of Ohmic Contacts. *ChemSusChem.* **2011**, *4*, 363–368.
39. Ibach, H. The Role of Surface Stress in Reconstruction, Epitaxial Growth and Stabilization of Mesoscopic Structures. *Surf. Sci. Rep.* **1997**, *29*, 195–263.
40. Baughman, R. H.; Cui, C.; Zakhidov, A. A.; Iqbal, Z.; Barisci, J. N.; Spinks, G. M.; Wallace, G. G.; Mazzoldi, A.; De Rossi, D.; Rinzler, A. G.; *et al.* Carbon Nanotube Actuators. *Science* **1999**, *284*, 1340.
41. Mathur, A.; Erlebacher, J. Size Dependence of Effective Young's Modulus of Nanoporous Gold. *J. Appl. Phys. Lett.* **2007**, *90*, 061910.